

A density-dependent failure criterion for concrete

Jan Arve Øverli*

*Department of Structural Engineering, Norwegian University of Science and Technology,
7491 Trondheim, Norway*

Abstract

This work focuses on the large effect of small secondary stresses on the compressive strength of concrete. The strength and especially the ductility of structural concrete members depend on local triaxial stress conditions that inevitably develop in the compressive zone just prior to failure. A failure criterion for concrete, which accounts for the effect of a reduced density of the concrete on the strength under fully compressive triaxial stress states, is proposed. The criterion was derived by curve-fitting mathematical expressions to axisymmetric strength data from a test programme on concretes of different weights previously published. For the purpose of evaluation, it was compared to other triaxial compressive strength data for lightweight aggregate concrete available in the literature; and to the failure criterion in fib Model Code 2010. It was found that, contrary to the Model Code criterion, the failure criterion presented in this paper generally provides safe lower bound estimates for the strength levels attained in the experimental tests.

Keywords: Lightweight aggregate concrete; failure criterion; short-term loading; generalised stress states; axisymmetric test data.

*Corresponding author

Email address: jan.overli@ntnu.no (Jan Arve Øverli)

1. Introduction

Lightweight aggregate concrete (LWAC) has been used as a construction material for many decades, with the main objective for using LWAC normally being to reduce the dead weight of structures. Thus, with a low weight, the dimensions of the foundations in buildings can be reduced in areas with low bearing capacities, while the inertia actions are reduced in seismic regions, and it also enables an easier handling and transportation of precast elements. Even with the major advantage of a reduced weight and the high strength-to-weight ratio of the material compared to conventional concrete, the use of LWAC is still limited as a mainstream construction material in the building industry. However, for large and advanced structures such as high-rise buildings, bridges and offshore structures, it has been applied with great success [1, 2, 3, 4, 5]. The major disadvantage of LWAC is the brittleness in compression at the material level compared to normal weight concrete (NWC). However, the strength and especially the ductility of structural concrete members depend on local triaxial stress conditions that inevitably develop in the compressive zone just prior to failure.

Today non-linear finite element analysis (NLFEA) is often used in design and verification of reinforced concrete structures. However, various analysts often obtain widely diverging results when modelling the same structure using the same FE code due to the uncertainty connected to many of the material parameters going into the analyses [6]. The response is significantly affected by parameters describing mechanisms such as: compression softening due to transverse cracking, confinement effects, tension softening, tension stiffening and rebar bond slip. There are two main reasons for this lack of generality and objectivity when the FE method is applied to concrete structures. Firstly, the material models employed by many analysts do not realistically describe

concrete as a material and, secondly, cracking of concrete may lead to numerical instabilities of the analyses if not adequate precautions are taken. In this respect it is interesting to note that remarkable good numerical results have been reported when applying a brittle triaxial material model which takes into account the increased transverse expansion of the concrete prior to failure [7]

The density dependent failure criterion presented in this paper was part of a research project where the goal was to get a better understanding of the ultimate behaviour of lightweight aggregate concrete at both the material and the structural level [8]. The working hypothesis was that the three key material characteristics generally dictating the ultimate response of concrete structures was: the large effect small secondary stresses have on the compressive strength; the abrupt increase of the transverse expansion at a stage close to, but not beyond, the peak stress level; and the rapid unloading of the material beyond the peak stress level. As a consequence of these features, the strength and especially the ductility of structural concrete members depend on local triaxial stress conditions that inevitably develop in the compressive zone just prior to failure rather than stress-redistributions owing to post-peak material characteristics as commonly believed. Confinement effects introduce the secondary stresses which increases the ductility of concrete as well as enhancing the concrete strength. Additionally, an active confinement from external stresses is more effective than a passive confinement, which is mobilized by an opposing transverse deformation from the Poisson effect. In reinforced concrete, the passive confinement from transverse reinforcement is the most common, and numerous researchers have investigated the effect of ordinary transverse steel reinforcement and the effect of adding fibres on the confinement in normal density concrete, both experimentally and theoretically [9, 10, 11]. For lightweight aggregate concrete, similar effects have been reported [12, 13, 14]. The hypothesis in this work has

previously been used with success to predict and explain the behaviour of normal weight concrete in the ultimate limit state [15, 16]. Hence, when applied to lightweight aggregate concrete, a failure criterion, which accounts for the effect of a reduced density on the strength under fully compressive triaxial stress states was needed.

Within structural concrete, the stresses frequently act in more than one direction [17, 18]. Hence, since the pioneering work of Richart, Brandtzæg and Brown [19], a large amount of research has been undertaken to describe the strength properties of concrete under combined states of stress. This has led to several acceptable formulations for the failure of concrete under general short-term loading. However, none of them account for the density of the concrete. Admittedly, the criterion implemented in fib Model Code 2010 (MC-10) [20] differentiates between normal weight concrete and lightweight aggregate concrete, although the density of the concrete is not a parameter. For normal density concrete the strength under multiaxial stress can be expressed with the uniaxial compressive strength since the failure can be considered as a function of the strength of the mortar. However, for lightweight concrete the influence of the aggregate must be taken into account since the failure can be governed by splitting of the aggregates. The most common and easiest available parameter for LWAC is the mass density of the concrete, which can be an input parameter in the formulation for the failure. Another option could be to make the failure dependent on e.g. the porosity of the aggregate.

Only a few researchers have examined the behaviour of LWAC under combined states of stress [21, 22, 23, 24, 25, 26, 27]. The most comprehensive investigation is a study performed by Hanson in 1963 [21], in addition a not so well-known test programme conducted at ‘Ente Nazioanale per l’Energia Elettrica’ (ENEL) in 1984 [26]. Since the latter forms the basis for the strength

criterion proposed in this paper and the results are not so easily accessible, it is briefly summarized in the next section.

2. The ENEL test programme

2.1. Experimental details

The result from this test programme were first presented at the 'International conference on concrete under multiaxial compression' held in Toulouse in 1984 [26]. The laboratory at ENEL was part of a joint test programme [28, 29] where it proved to provide reliable results. Four different types of concretes were examined: one heavyweight, one normalweight and two types of LWAC. The composition of the mortar was the same for all concretes, i.e. only the weight of the coarse aggregate particles varied. For all concretes, approximately 40% of the total volume consisted of coarse aggregate, while the remaining 60% of the volume was occupied by the mortar. The observed differences in strength and deformational behaviour could therefore solely be attributed to the properties of the aggregate. The heavyweight aggregate was a crushed mineral with a high specific density (Barite); the normal weight aggregate was from a natural source of alluvial gravels (Vailata), while the lightweight aggregate was either sintered pulverized fuel-ash (Lytag) or expanded clay (Leca). The details of the mix design are given in Table 1. The total weight and the uniaxial compressive strengths established from the triaxial compression tests with zero confining pressure are also included in the table.

The strength and deformational behaviour under axisymmetric triaxial compression were studied by bringing 100 mm of cubical specimens to failure by following two different load paths: a hydrostatic loading up to a predetermined load level with a subsequent increase of the stress in either the vertical direction (triaxial compression) or equally in the two horizontal directions (triaxial ex-

Table 1: Composition of the different concretes and the reference mortar utilized in the test programme [26].

	Barite (kg/m^3)	Vailata (kg/m^3)	Lyttag (kg/m^3)	Leca (kg/m^3)	Mortar (kg/m^3)
Portland cement 425	350	350	350	350	583
Effective water	175	175	175	175	292
Absorbed water	-	-	80	45	-
Sand	700	700	700	700	1167
Aggregate (8 – 15 mm)	1850	1150	625	250	-
Total weight (kg/m^3)	3075	2375	1930	1520	2042
Concrete strength (MPa)	41.6	40.2	38.7	15.5	44.5

tension). The load was applied through steel platens, which were lubricated by polyethylene sheets with grease in-between to minimize friction, a test method that has earlier been proven to provide reliable results [28, 29]. Four different confining stress levels were examined for each load path, with three replications of each, resulting in a total number of 120 test specimens in the test program. Obviously, a confining stress level equal to zero leads to the special cases; uniaxial compression and equibiaxial compression for load path 1 and load path 2 respectively.

2.2. Experimental strength data

Figure 1 depicts the strength data from the triaxial compression tests (upper points) and the triaxial extension tests (lower points), with the data normalized by the uniaxial compressive strength f_c (established from the triaxial compression tests with zero confining pressure). Every strength value is the mean of three tests conducted after 56 days of curing [26].

Normalized results usually leads to strength data that tend to fall onto a single curve. This is a very convenient feature, since it allows the failure envelopes to be singly expressed as a function of f_c . However, as the density of the concrete decreases, the envelopes deviate toward the hydrostatic axis. Hence, in order to capture the behaviour of the lightweight concretes, the effect of the increased porosity of the aggregates must somehow enter into the expressions.

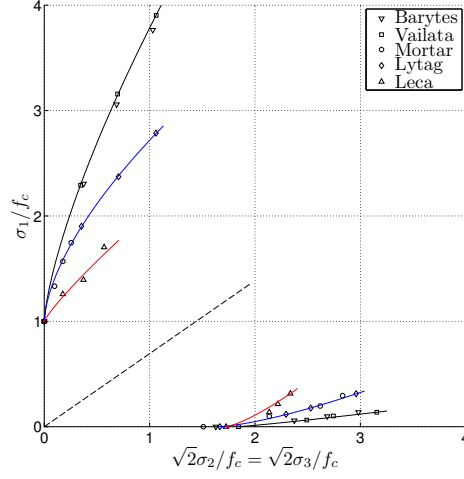


Figure 1: Strength data in the axisymmetric stress plane.

Failure envelopes are often described mathematically by the variation of the axial stress σ_1/f_c as a function of the confining stress $\sigma_2/f_c = \sigma_3/f_c$. The ENEL researchers followed this tradition and proposed the following equations for the upper and lower set of curves respectively.

$$\frac{\sigma_1}{f_c} = 1 + k_1 \left(\frac{\sigma_2}{f_c} \right)^{k_2} \quad (1)$$

$$\frac{\sigma_1}{f_c} = \left[\frac{1}{k_3} \left(\frac{\sigma_2}{f_c} - k_5 \right) \right]^{k_4} \quad (2)$$

The parameters k were chosen as functions of the porosity of the aggregates through second-degree polynomial expressions. It is interesting to note the resemblance of Equation 1 to the linear expression $\sigma_1/f_c = 1 + 4.1(\sigma_2/f_c)$ proposed by Richart, Brandtæg and Brown as the main outcome of their classical triaxial cylinder tests [19]. The second constant k_2 , added by the ENEL researchers take on values below 1.0 and, thus allow for the curvature of the envelopes towards the hydrostatic axis.

2.3. Experimental deformational data

Figure 2 depicts the deformational data from the triaxial compression tests (solid lines) and the triaxial extension tests (dotted lines). The deformational data stem from the same tests that led to the strength data in Figure 1. The results are presented as the the volume variation $\Delta V/V$ versus the applied stress σ (normalized by the stress at failure f_u). The figure presents curves for each aggregate at four different confining stress levels. The maximum confining stresses are 75% of the uniaxial compressive stress for the triaxial compression tests and 30% for the triaxial extension tests. In Figure 2 there is an increase in the initial hydrostatic stress level from left to right. The far left unbroken and dashed curves represent the special cases of uniaxial and equibiaxial compression, respectively. As expected, the volume compaction increases with an increasing stress level. However, it is more interesting to note that as the porosity of the aggregate decreases, there is a tendency towards a continuous volume compaction of the concrete. This is in contrast to the dense aggregate concretes, for which the initial volume compaction is always followed by a subsequent volume expansion, even for the fully compressive triaxial stress states. Hence, for concretes with porous aggregates, the triaxial compressive strength may be limited by the crushing of the aggregate. As a result, the failure surface in the stress space will be close-ended. This can be modelled by introducing a cap function in the description of the failure surface. Nevertheless, its shape and intersection with the hydrostatic axis can not currently be assessed since there is no triaxial compressive strength data for LWAC in the lower density range or in the upper density range under moderate-to-high confining pressures, for which this may become relevant.

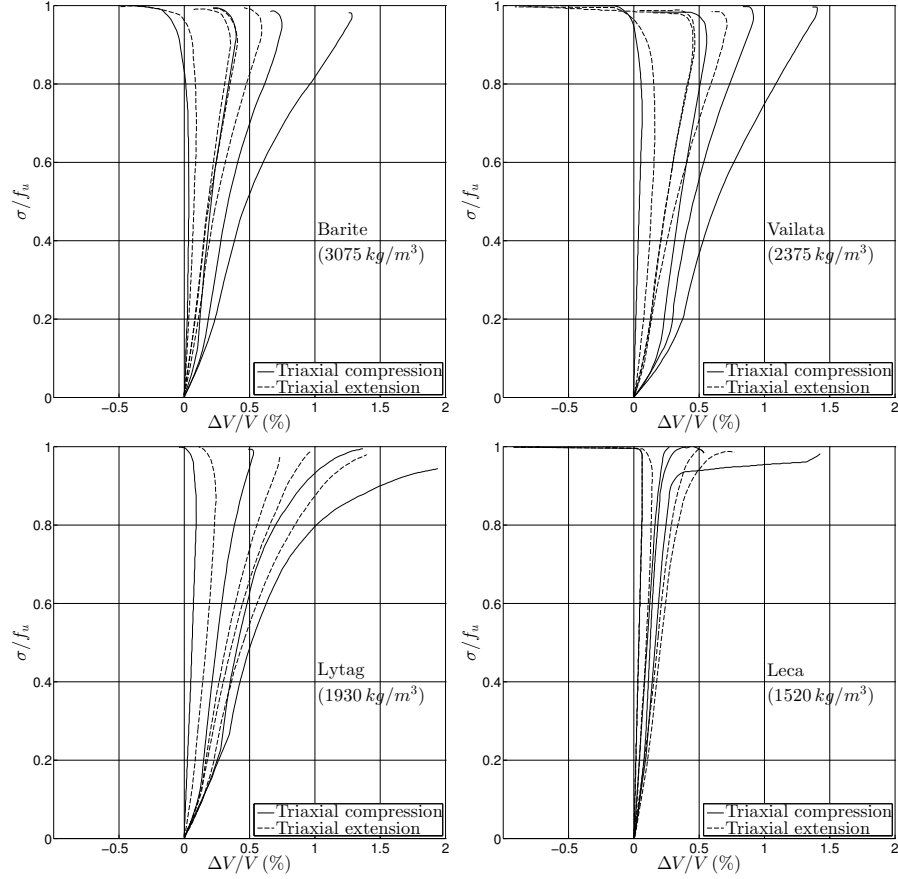


Figure 2: Deformational data presented as the volume variation versus the applied stress normalized by the failure stress.

3. Failure criteria for concrete

3.1. The underlying theory

When establishing a failure criterion for concrete, it is usually assumed that the material is homogeneous and isotropic. For an isotropic material, a general state of stress $(\sigma_x, \sigma_y, \sigma_z, \tau_{xy}, \tau_{xz}, \tau_{yz})$ can uniquely be defined by the principal stresses $(\sigma_1, \sigma_2, \sigma_3)$. Because the principal stresses are independent of the coordinate system, they could in theory form the basis for the description of the failure surface. However, for computer applications the failure criterion can

conveniently be translating the stress state into its hydrostatic and deviatoric components as shown in Figure 3.

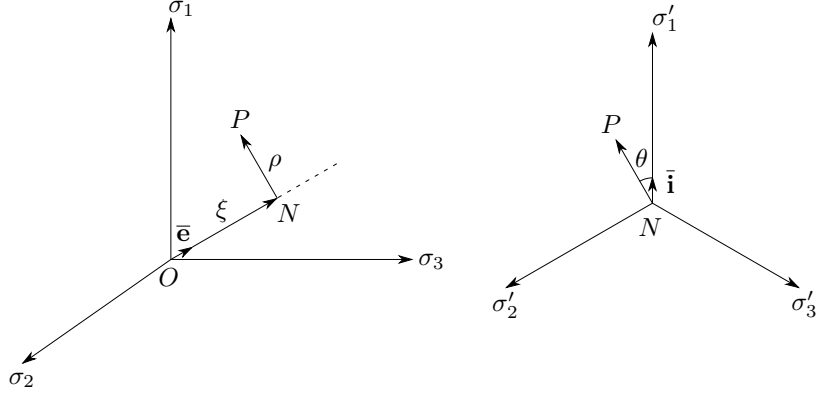


Figure 3: Relationship between the Cartesian coordinates $(\sigma_1, \sigma_2, \sigma_3)$ and the octahedral coordinates (ξ, ρ, θ) .

It can be seen that alternatively to the normal Cartesian coordinates $(\sigma_1, \sigma_2, \sigma_3)$, the stress state P can be described by a vector $\overline{\mathbf{ON}}$ lying on the hydrostatic axis, a vector $\overline{\mathbf{NP}}$ on the deviatoric plane, and the angle θ of the latter vector on the deviatoric plane. The lengths of the vectors are given by

$$\xi = |\overline{\mathbf{ON}}| \cdot \bar{\mathbf{e}} = \frac{1}{\sqrt{3}} I_1 \quad \text{and} \quad \rho = \sqrt{|\overline{\mathbf{NP}}| \cdot |\overline{\mathbf{NP}}|} = \sqrt{2J_2} \quad (3)$$

Further, the trigonometrical identity $\cos 3\theta = 4 \cos^3 \theta - 3 \cos \theta$, combined with the relation $\overline{\mathbf{NP}} \cdot \bar{\mathbf{i}} = \rho \cos \theta$, yields the following expression for the rotational variable θ on the deviatoric plane

$$\cos 3\theta = \frac{3\sqrt{3}J_3}{2J_2^{3/2}} \quad (4)$$

In the above equations, I_1 is the first invariant of the stress tensor and J_2 and J_3 are the second and third invariants of the deviatoric part of the stress tensor. Moreover, as an alternative to represent the failure criterion in the principal stress space, the octahedral stress space is often used as a coordinate system. The hydrostatic and deviatoric components of the stress tensor are then expressed in terms of the normal octahedral stress σ_o and shear octahedral stress τ_o , which are defined as

$$\sigma_o = \frac{\xi}{\sqrt{3}} \quad \text{and} \quad \tau_o = \frac{\rho}{\sqrt{3}} \quad (5)$$

Since concrete may be considered to be isotropic before the failure surface is attained, i.e. six-fold symmetry of the failure surface can be assumed, the strength data from these load paths is sufficient to fully define the deviatoric plane. Hence, if such strength data are determined for an adequate number of hydrostatic stress levels, mathematical expressions for the entire failure surface can be derived. Meridians represents the intersection curves between the failure surface and a plane containing the hydrostatic axis with θ being constant. The state of stress on the meridians have two equal principal stresses. On the compressive meridian ($\theta = 60^\circ$) they are greater than the third, on the tensile meridian ($\theta = 0^\circ$) they are smaller.

The advantage of adopting an octahedral formulation of the material data is that the same relations can be used to express uniaxial, biaxial and triaxial concrete behaviour, i.e. the material model can be used to describe the behaviour of concrete under generalised states of stress [29]. The strength and constitutive relations are obtained directly by fitting curves to material data from multiaxial tests. Obviously, this requires a lot of testing at the material level. However, for concrete, this seems to be the best option since, as stated in

the CEB-FIP state of the art report on finite element modelling of reinforced concrete structures [6], ‘concrete is a complex and stubborn material that sometimes refuses to act according to accepted rules of mechanics’. Hence, it can be argued that empirical fitted curves are to prefer over the classical continuum mechanics formulations, since the latter seems to be to much of a straightjacket for the mathematical descriptions and, moreover, does not seem to provide a sound theoretical foundation for the material behaviour.

3.2. Octahedral representation of the strength data

Figure 4 shows the failure envelopes from the ENEL test programme in the octahedral stress plane, thus, the strength data have been replotted in terms of σ_o and τ_o . From this kind of representation, it can clearly be seen that the compressive meridian and the tensile meridian of the failure surface generally do not coincide, with the tensile meridian normally being closer to the hydrostatic axis. This indicates that the strength of concrete not merely is a function of the state of stress at failure (σ_o, τ_o) , but also depends on the load path taken to reach that particular combination of stresses. However, as the hydrostatic stress component increases and the density of the concrete decreases, the envelopes tend toward a single curve. This means that the state of stress at failure become less dependent on the rotational variable θ , i.e. the shape of the deviatoric plane becomes more circular. This is probably due to the strength being limited by the compressibility of the aggregate. The deformational data from Figure 2 supports this. For the normalweight and the heavyweight concrete, where the mortar governs the overall behaviour, the initial volume compaction of the material was always followed by subsequent volume dilation before failure, also for fully compressive triaxial stress states. However, as the weight of the aggregate decreased and the hydrostatic stress level increased, a stage was eventually reached where there was no volumetric strain reversal before failure, which clearly indicates

a collapse of the aggregate phase. Hence, it may be sufficient to test for only axi-symmetric states of stress, or maybe even only the ‘compressive’ ones. It should be reminded that by ‘compressive’ ones is meant the entire ‘compression’ meridian, which includes both the T-T-C (Tension-Tension-Compression) and the C-C-C regime. In this respect, it is also convenient to be aware of the fact that the T-T-C or the T-C-C regime of concrete generally tend to be quite similar [15].

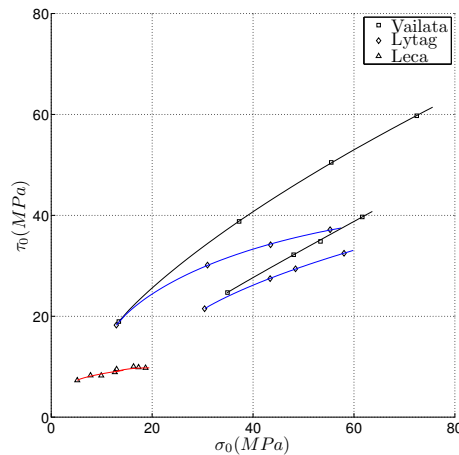


Figure 4: Failure envelopes in the octahedral stress plane.

3.3. The density-dependent failure criterion

The proposed density-dependent failure criterion in this work [30], is a modification of the criterion proposed by Kotsovos [31]. By decomposing the response of biaxially and triaxially loaded test specimens into octahedral stresses and strains, simple expressions for secant and tangent bulk and shear moduli were developed which are only dependent on stress level and compressive strength. Assumptions in this model were that the deviatoric deformation due to pure hydrostatic loading is negligible and pure deviatoric loading results in both deviatoric and volumetric deformation [15]. The state of strain corresponding to

any state of stress can thus be calculated from Hookes law using the secant moduli for that particular state of stress and a coupling term for the volumetric response to deviatoric loading. The simple expressions for the failure surface are given for the the compressive meridian ($\theta = 60^\circ$) and the tensile meridian ($\theta = 0^\circ$) as

$$\frac{\tau_{oc}}{f_c} = k_1 \left(\frac{\sigma_o}{f_c} + 0.05 \right)^{k_2} \quad \text{where } k_1 = 0.944, k_2 = 0.724 \quad (6)$$

$$\frac{\tau_{oe}}{f_c} = k_3 \left(\frac{\sigma_o}{f_c} + 0.05 \right)^{k_4} \quad \text{where } k_1 = 0.633, k_2 = 0.857 \quad (7)$$

Furthermore, the meridians for any θ intermediate between 0° and 60° may be described by the interpolating function given in Equation 8 [32]. Hence, once the variations of τ_{oc} and τ_{oe} with σ_o are determined, the entire failure surface is defined (assuming six-fold symmetry, i.e. isotropic behaviour).

$$\tau_{ou} = \frac{2\tau_{oc}(\tau_{oc}^2 - \tau_{oe}^2) \cos \theta + \tau_{oc}(2\tau_{oe} - \tau_{oc}) \sqrt{4(\tau_{oc}^2 - \tau_{oe}^2) \cos^2 \theta + 5\tau_{oe}^2 - 4\tau_{oc}\tau_{oe}}}{4(\tau_{oc}^2 - \tau_{oe}^2) \cos^2 \theta + (\tau_{oc} - 2\tau_{oe})^2} \quad (8)$$

For both the heavyweight and normal weight concrete, the curves are drawn according to Equations 6 and 7 without modifications. However, in order to capture the behaviour of the two lightweight concretes, the constants in the expressions were made functions of the density of the concrete ρ through second degree polynomial expressions. A regression analysis led to the following relationships:

$$k_1(\rho) = -5.7378 \cdot 10^{-9} \rho^2 + 0.0003710 \rho + 0.0866$$

$$k_2(\rho) = -1.1194 \cdot 10^{-7} \rho^2 + 0.0009045 \rho - 0.8020$$

$$k_3(\rho) = -6.5941 \cdot 10^{-8} \rho^2 + 0.0003387 \rho + 0.1999$$

$$k_4(\rho) = -3.5656 \cdot 10^{-7} \rho^2 + 0.0018014 \rho - 1.4125$$

These parameters are only valid in the fully compressive region of the failure surface. In the tensile regions, it is assumed that Equations 6 and 7 can be used in their original form due to a lack of relevant experimental data. Figure 5 compares strength data to the proposed density-dependent failure criterion in the octahedral stress space, showing the difference in the compressive and tensile meridian.

In Figure 6, the failure envelopes in the axisymmetric stress plane are presented together with the corresponding complete failure surfaces in the three-dimensional stress space. In order to close the surfaces in tension, the tensile hydrostatic stress is limited to $0.05f_c$. As seen in the figure the shape of the failure surface in the deviatoric plane changes from almost triangular for low hydrostatic stresses to approximately circular with increasing hydrostatic pressure.

3.4. The failure criterion in Model Code 2010

The failure criterion employed in fib Model Code 2010 (MC-10) is based on the Ottosen criterion [33] and is given by the equation

$$\alpha \frac{J_2}{f_c^2} + \lambda \frac{\sqrt{2}}{f_c} + \beta \frac{I_1}{f_c} = 0 \quad (9)$$

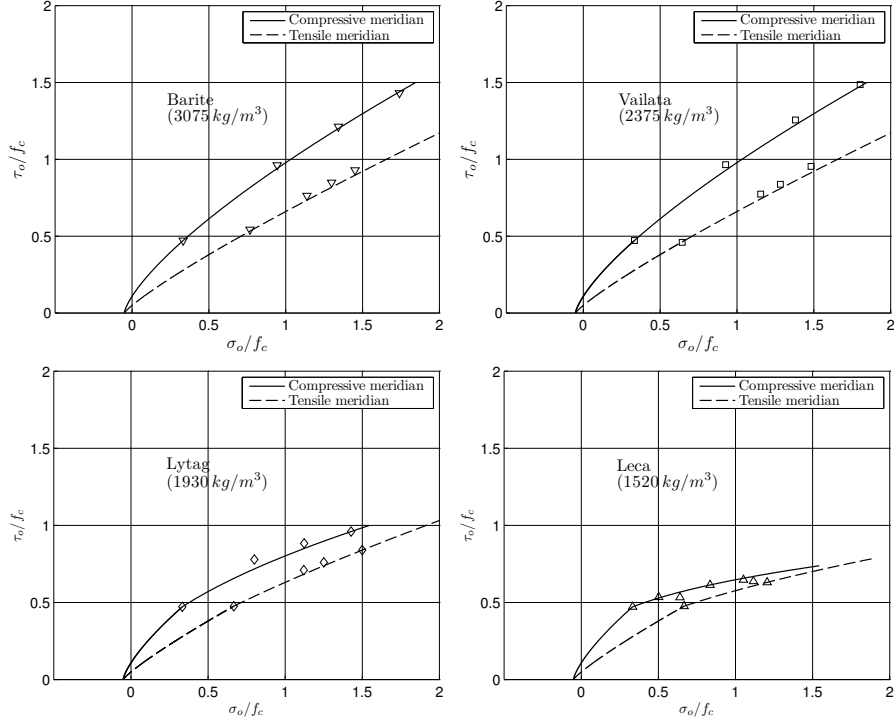


Figure 5: Comparison of strength data to the proposed density-dependent failure criterion.

where the function λ depends on the deviatoric angle θ through the expression

$$\lambda = c_1 \cdot \cos \left[\frac{1}{3} \cdot \arccos(c_2 \cdot \cos 3\theta) \right] \quad (10)$$

The factors α , β , c_1 and c_2 are material parameters assessed such that the criterion fit the uniaxial compressive strength, the uniaxial tensile strength, the biaxial compressive strength and a failure state $(\sigma_o/f_c, \tau_o/f_c) = (x, y)$ along the compression meridian. In the original calibration the biaxial compressive strength was taken as $1.16 \times f_c$ and the compression meridian was fitted to pass through the point $(-2.89, 2.31)$ (note that contrary to Figure 5, tensile

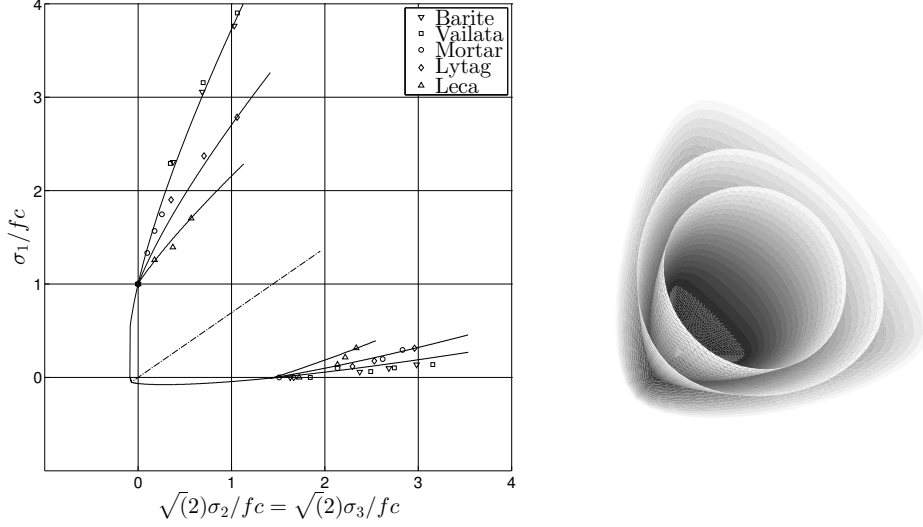


Figure 6: Failure envelopes in the axisymmetric stress plane according to the proposed density-dependent octahedral expressions together with the corresponding complete failure surfaces.

stresses are defined as positive). However, in MC-10 these values have been made functions of f_c . The biaxial compressive strength is taken as $(1.2 - 0.001f_c) \times f_c$, whereas the fitting point on the compression meridian is given for NWC and LWAC by:

$$(\sigma_0, \tau_0) = \left(-240, 185 - 180 \frac{f_c}{100} + 260 \frac{f_c^2}{100} - 84 \frac{f_c^3}{100} \right) \quad (11)$$

$$(\sigma_0, \tau_0) = \left(-60, 250 \frac{f_c}{100} - 460 \frac{f_c^2}{100} + 310 \frac{f_c^3}{100} \right) \quad (12)$$

In Figure 7, the MC-10 criterion is compared to the proposed density-dependent failure criterion. The tensile strength is chosen as $0.05 \times f_c$ in the MC-10 criterion in an attempt to match the tensile regions of the two criteria. It can be seen that the two criteria are quite similar, but that the MC-10 criterion overestimates the strength in triaxial compression for both NWC and LWAC.

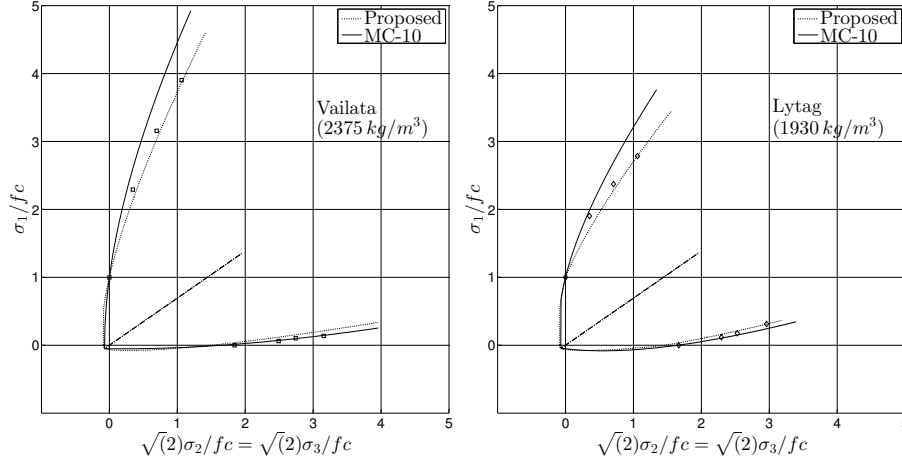


Figure 7: The failure criterion in MC-10 and the proposed density-dependent criterion compared to the strength data from the ENEL tests.

3.5. Comparison with other experimental data

It is not surprising that the proposed density-dependent criterion fits the data used for its calibration. Hence, in Figure 8, the two criteria are compared to other axisymmetric triaxial strength tests for LWAC performed by Niwa et al. [22], Hobbs [25] and Hanson [21]. Contrary to the MC-10 criterion, it can be seen that the proposed density-dependent criterion provide safe lower bound values to all strength data. However, it is interesting to note from the Hanson tests that if rounded lightweight aggregates with a dense outer shell are used (black dots in the figure), the strength becomes more in accordance with the MC-10 criterion and seems to depend less on the density, at least for the stress levels examined in the tests.

4. Discussion

The strength of LWAC is governed by the properties of the mortar and the aggregate and their interaction. In the ENEL test programme, the mortar was kept constant, while the density of the coarse aggregate particles varied.

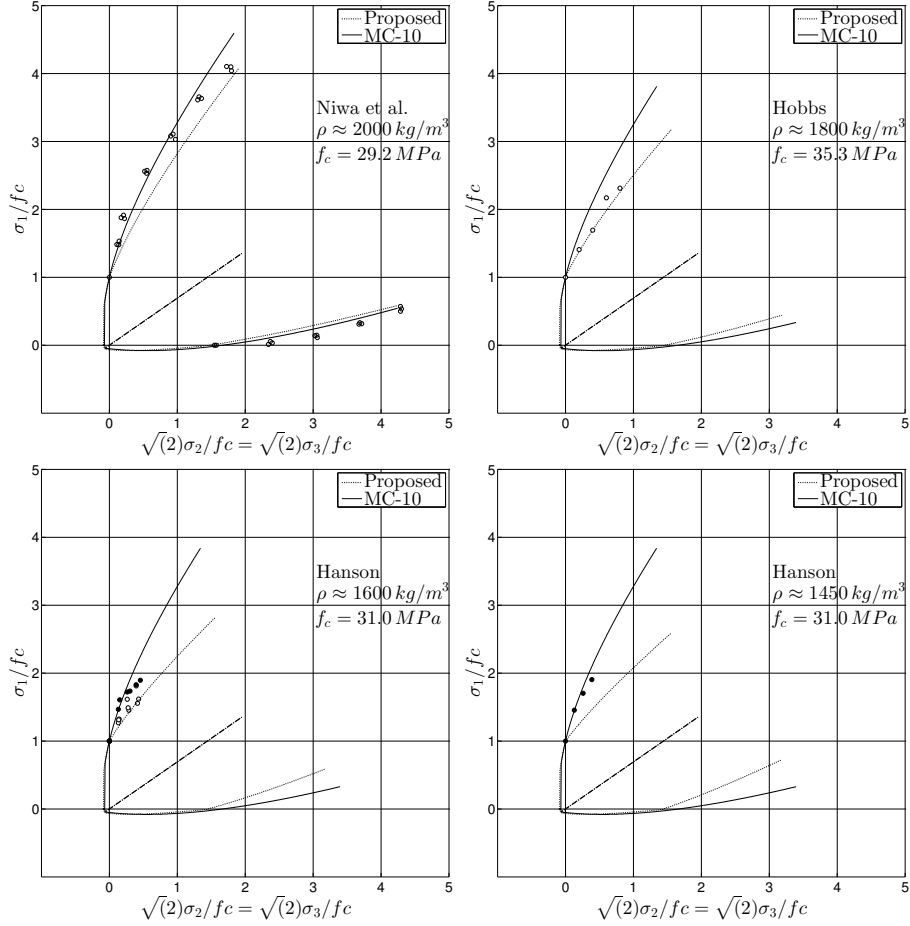


Figure 8: Strength data in the axisymmetric stress plane according to tests

Nonetheless, in the Hanson tests the uniaxial compressive strength was kept constant while the type of coarse aggregate particles varied. From Figure 8, it can be seen that aggregates producing similar concrete density may lead to a varying triaxial compressive strength, in which aggregates with a smooth dense outer shell seem to perform better than aggregates with a porous surface. This is probably due to an enhanced aggregate/mortar bond for the latter, since the surfaces of a porous or pozzolanic character tend to improve the bond [34]. This may have enabled these concretes to obtain the desired uniaxial compressive

strength with a weaker mortar, as the aggregate will then have to take a greater share of the load under triaxial compression.

Some researchers have suggested that the strength gain under triaxial compression is a result of microcracks of a random orientation developing under hydrostatic compression [35]. They act so as to inhibit the crack propagation under subsequent deviatoric loading through the Cook-Gordon crack-stopping mechanism [36]. Because increased aggregate/mortar bond results in a lower degree of microcracking, this effect will diminish for the concretes with aggregates with a porous surface. However, the concretes with aggregates with a dense outer shell could behave more like a NWC. In fact, if the aggregates are stronger and stiffer than the mortar, there might be no difference at all, since the transfer of internal forces will be similar to that of a normal dense concrete (see Figure 9). This implies that it is not merely the density that is impor-

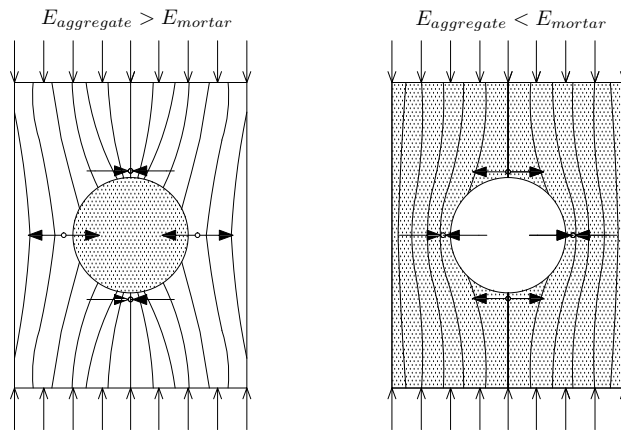


Figure 9: Internal stress transfer in concrete under a compressive load for either: a stiffer and stronger aggregate embedded in a softer and weaker mortar; or a softer and weaker aggregate embedded in a stronger and stiffer mortar [37].

tant, but also the relative strength of the concrete compared to the density. Hence, if a strong lightweight aggregate is used to produce an LWAC of modest strength, the behaviour might correspond to that of an NWC [38], at least when

an aggregate with a dense outer shell is used. However, if a light, and thereby weak, aggregate is used to produce an LWAC of high strength (possibly utilizing the excellent bond characteristics of a lightweight aggregate with a porous and pozzolanic surface), a very low triaxial strength gain is expected since the aggregate will then be pushed to its limit even without a confining pressure, and the amount of microcracking will then be reduced to a minimum.

5. Conclusions

A failure criterion for concrete, which accounts for the effect of reduced density on the triaxial compressive strength, has been proposed. The criterion was derived by curve-fitting previously existing mathematical expressions for NWC [31] to axisymmetric strength data for concretes of varying density [26]. Contrary to the MC-10 criterion [20], the proposed density-dependent criterion was found to provide safe lower bound estimates of the other triaxial compressive strength data for LWAC reported in the literature [21, 22, 25]. It should nonetheless be noted that such data are scarce, and more data is needed to refine the criterion, e.g. with the inclusion of a cap function. Moreover, no data exists for tensile regions of the failure surfaces, which led to the (probably erroneous) assumption that these were similar to that of NWC. It is also important to realise the complexity involved in defining a failure criterion for concrete. This work is limited by taking into account only the density of the concrete in the formulation. The type of aggregate influences highly the bond between aggregate and mortar and plays an important role in distribution of the internal stresses in the concrete. In some cases this factor can be more relevant than the density of the aggregate.

Acknowledgments

Most of this work is based on the PhD thesis of Håvard Nedreliid from the Norwegian University of Science and Technology. Sadly, he passed away in 2015. In his memory the author hopes he has been able to present the work with the respect and quality it deserves. The work was carried out with financial support from COIN, the Concrete Innovation Centre, which was a centre for research-based innovation with funding from the Research Council of Norway and industrial partners in the period 2006-2014.

References

- [1] fib Bulletin 8, Lightweight aggregate concrete, Federation Internationale du Beton, Lausanne, Switzerland, 2000.
- [2] A. Haug, S. Fjeld, A floating concrete platform hull made of lightweight aggregate concrete, *Engineering Structures* 18 (1996) 831 – 836.
- [3] T. Ingebrigtsen, Stolma bridge norway, *Structural Engineering International* 9 (1999) 100–102.
- [4] Adriatic LNG Terminal, <http://www.edison.it/en/adriatic-lng-terminal>, 2008. Accessed: 2016-06-23.
- [5] Harpe bridge, <http://www.tu.no/artikler/denne-brua-kan-ikke-bygges-med-norsk-stein/230834>, 2015. Accessed: 2016-06-23.
- [6] fib Bulletin 45, Practioner’s guide to finite element modellering of reinforced concrete structures, Federation Internationale du Beton, Lausanne, Switzerland, 2008.

- [7] F. Vidosa, M. Kotsovos, M. Pavlovi, Nonlinear finite-element analysis of concrete structures: Performance of a fully three-dimensional brittle model, *Computers & Structures* 40 (1991) 1287 – 1306.
- [8] COIN, Concrete Innovation Centre, Focus Area 3.3: Structural performance, www.coinweb.no, 2007-2015.
- [9] H. Cheong, H. Zeng, Stress-strain relationship for concrete confined by lateral steel reinforcement, *ACI Materials Journal* 99 (2002) 250–255.
- [10] J. B. Mander, M. J. N. Priestley, R. Park, Observed stress-strain behavior of confined concrete, *Journal of Structural Engineering* 114 (1988) 1827–1849.
- [11] M. Attard, S. Setunge, Stress-strain relationship of confined and unconfined concrete, *ACI Materials Journal* 93 (1996) 432–442.
- [12] P. Balaguru, A. Foden, Properties of fiber reinforced structural lightweight concrete, *ACI Structural Journal* 93 (1996) 62–78.
- [13] G. Campione, L. L. Mendola, Behavior in compression of lightweight fiber reinforced concrete confined with transverse steel reinforcement, *Cement and Concrete Composites* 26 (2004) 645 – 656.
- [14] J. A. Overli, T. M. Jensen, Increasing ductility in heavily reinforced LWAC structures, *Engineering Structures* 6263 (2014) 11 – 22.
- [15] M. Kotsovos, M. Pavlovic, *Structural concrete: Finite-element analysis for limit-state design*, Thomas Telford Ltd, 1995.
- [16] M. Engen, M. A. N. Hendriks, J. A. Overli, E. Aldstedt, Solution strategy for non-linear finite element analyses of large reinforced concrete structures, *Structural Concrete* 16 (2015) 389–397.

- [17] D. W. Hobbs, C. Pomeroy, J. B. Newman, Design stresses for concrete structures subject to multi-axial stresses, *The Structural Engineer* 55 (1977) 151–164.
- [18] M. D. Kotsovos, Consideration of triaxial stress conditions in design: a necessity, *ACI Structural Journal* 84 (1987) 266–273.
- [19] F. E. Richart, A. Brandtzæg, R. L. Brown, A study of the failure of concrete under combined compressive stresses, Technical Report Bulletin 185, University of Illinois, Engineering Experimental Station, Champaign, Illinois, 1928.
- [20] fib, Model code 2010 - first complete draft, Federation Internationale du Beton, Lausanne, Switzerland, 2010.
- [21] J. Hanson, Strength of structural lightweight concrete under combined stress, *Journal of the Portland Cement Association* January (1963) 39–45.
- [22] Y. Niwa, S. Kobayashi, W. Koyanagi, Failure criterion of lightweight aggregate concrete subjected to triaxial compression, *Transactions of the Japan Society of Civil Engineers* 143 (1966) 28–35.
- [23] M. A. Taylor, A. k. Jain, M. R. Ramey, Path dependent biaxial compressive testing of an all-lightweight aggregate concrete, *ACI Journal Proceedings* 69(12) (1972) 758–764.
- [24] Y. Atan, F. O. Slate, Structural lightweight concrete under biaxial compression, *ACI Journal Proceedings* 70(3) (1973) 182–186.
- [25] D. Hobbs, Failure criteria for concrete, *Handbook of structural concrete* (ed. Kong) 87 (1983) 10–1–10–40.

- [26] M. Berra, A. Faticciono, G. Ferrara, Triaxial behaviour of concretes of different weights, Proceedings - International Conference on Concrete under Multiaxial Conditions, Volume 1 (1984) 176–189.
- [27] A. Hussein, H. Marzouk, Behavior of high-strength concrete under biaxial stresses, ACI Materials Journal 97 (2000) 27–36.
- [28] K. H. Gerstle, D. L. Linse, P. Bertacchi, Strength of concrete under multiaxial stress states, ACI special publication SP-55 (1978) 103–131.
- [29] K. H. Gerstle, H. Aschl, R. Belotti, P. Bertacchi, M. D. Kotsovos, H.-Y. Ko, D. Linse, J. B. Newman, P. Rossi, G. Schickert, M. A. Taylor, L. A. Traina, H. Winkler, R. M. Zimmerman, Behavior of concrete under multiaxial stress states, Journal of the Engineering Mechanics Division 106 (1980) 1383–1403.
- [30] H. Nedrelid, Towards a better understanding of the ultimate behaviour of lightweight aggregate concrete in compression and bending, Ph.D. thesis, Norwegian University of Science and Technology, 2012.
- [31] M. D. Kotsovos, A mathematical description of the strength properties of concrete under general stress, Magazine of concrete research 31 (1979) 151–158.
- [32] K. J. Willam, E. P. Warnke, Constitutive model for the triaxial behaviour of concrete, Seminar on Concrete Structures Subjected to Triaxial stresses (1974) Paper III-1.
- [33] N. S. Ottosen, A failure criterion for concrete, Journal of the Engineering Mechanics Division 103 (1977) 527–535.
- [34] S. Chandra, L. Berntsson, Lightweight aggregate concrete - Science, Technology and applications, William Andrew Publishing/Noyes, 2002.

- [35] M. D. Kotsovos, Fracture processes of concrete under general stress states, *Materials and Structures* 12 (1979) 431–437.
- [36] J. Cook, J. E. Gordon, A mechanism for the control of crack propagation in all-brittle systems, *Proceedings of the Royal Society of London A* 282 (1964) 508–520.
- [37] B. K. Bardhan-Roy, W. F. G. Crozier (Eds.), *FIP Manual of lightweight aggregate concrete* (2. ed.), Surrey University Press, 1983.
- [38] M. E. R. Little, The use of lightweight aggregate for structural concrete, *The Structural Engineer* 55 (1977) 539–546.